nature communications

Article

https://doi.org/10.1038/s41467-025-67012-z

Graded encoding of spatial novelty scales in the human brain

Received: 1 April 2025

Accepted: 19 November 2025

Published online: 04 December 2025

Check for updates

Jörn A. Quent[1,2], Liangyue Song[1], Xinyu Liang[1], Yueting Su[1], Wenwen Yu[1,3], He Wang[1,3] & Deniz Vatansever[1,3]

Successful navigation relies on the ability to process and encode detailed information about our dynamic environments. Beyond familiarity, emerging studies now highlight the crucial role of novelty detection in this process, the precise neural mechanism of which remains poorly understood. Using ultra-high field 7T fMRI, we investigated how the human brain encodes spatial novelty during virtual navigation, with a particular focus on graded representations that follow systematic transitions between novel and familiar spaces. Our results revealed novelty and familiarity specific neural responses within the posterior and anterior poles of the bilateral hippocampus, respectively. On the cortical surface, two separable streams of activity patterns were observed in which regions within the visual and frontoparietal networks showed novelty-specific activity, while somatomotor, ventral attention and default mode regions preferred spatial familiarity. Importantly, we identified a distinct gradient along the hippocampal long axis and demonstrated the extended contribution of the posterior medial cortex to the encoding of spatial novelty scales that were intrinsically coupled with the hippocampal gradient. These findings advance our understanding of how the human brain encodes and processes spatial information, suggesting that graded representations of spatial novelty may serve as a fundamental organizational principle for spatial cognition in the human brain.

In parallel with other animal species, humans possess a remarkable capacity for encoding detailed spatial information about their dynamic and complex environments. As we explore and interact with our surroundings, we gradually develop cognitive maps that enable us to navigate efficiently and plan goal-directed actions[1–3]. This spatial cognitive ability not only enhances related skills such as object manipulation and visualisation[4], but is also crucial for healthy brain function, with its impairment showing notable links to memory disorders[5–8].

While environmental familiarity undoubtedly influences how we use spatial representations[9–11], emerging studies now indicate that novelty may also play an equally important role in effective navigation[12]. The detection of novelty, particularly when it deviates from expectations, serves as a powerful learning signal that enhances memory formation[13]. At the neural level, prior neuroimaging studies have demonstrated increased hippocampal activity in response to spatial novelty[12,14,15]. In addition to the recognised importance of the hippocampus in the formation, maintenance and use of cognitive maps for the neural representation of our spatial environments[16], a potential role for this medial temporal lobe structure in the encoding of spatial novelty aligns with its observed sensitivity to novelty and surprise in other contexts, such as the detection of new or irregular images or unexpected sequences[17–19]. Nevertheless, despite the emerging importance ascribed to spatial novelty for effective navigation[20–22], our understanding of the neural encoding mechanism of this process within the complex functional organisation of the human brain remains limited, requiring further investigation[22,23].

[1]Institute of Science and Technology for Brain-inspired Intelligence, Fudan University, Shanghai, China. [2]MOE Frontiers Centre for Brain Science, Fudan University, Shanghai, China. [3]Zhangjiang International Brain Imaging Centre, Fudan University, Shanghai, China. e-mail: deniz@fudan.edu.cn

While the hippocampus maintains a relatively uniform internal circuitry[24,25], a pattern of graded differentiation has consistently been observed along its anterior-to-posterior axis in humans (analogous to the ventral-to-dorsal axis in rodents[26,27]), which may potentially serve as a key organisational mechanism for encoding environmental relations. These hippocampal gradients encompass various intrinsic features, including connectivity patterns, receptor distribution, tau pathology and gene expression profiles, as well as informational content[26–29]. Furthermore, representations like increasing receptive fields of rodent place cells appear to facilitate effective coding of environments for goal-directed behaviour[25]. In humans, similar gradients were identified for visual processing[30], for ongoing cognition at rest[31,32] and during spatial navigation[32–34], with recent evidence alluding to the potential preservation of this coding mechanism through evolutionary expansion[35].

Importantly, these spatial processing gradients in humans have been shown to extend beyond the hippocampus into neocortical regions, such as the posterior medial cortex[36], indicating a broader role for the gradient-based encoding of spatial information in the human brain. Recent studies suggest that such gradients may reflect a fundamental macro-scale organisational principle across multiple cognitive domains[37]. For example, anterior parts of the retrosplenial cortex and parahippocampal place area have been shown to encode successively wider temporal representations[38], while gradients spanning regions within the default mode and frontoparietal networks are suggested to correlate with changes in long-term memory demands during semantic processing[37,39]. In the context of spatial representations, the posterior medial cortex demonstrates a gradient of spatial scales ranging from local (e.g. rooms) to global (e.g. continents) that mirrors the hippocampal organisation[36]. Together, converging evidence suggests that graded representations may constitute a key encoding mechanism for the neural representation of knowledge in the human brain, including spatial information[40].

In this study, our main objective was to investigate the neural mechanisms underlying the processing of spatial novelty during naturalistic virtual navigation. Based on prior evidence[41,42], we hypothesised that spatial novelty-to-familiarity follows a graded representation across both the hippocampus and extra-hippocampal brain regions. Using ultra-high field 7T fMRI, we recorded brain activity as participants actively explored a virtual reality environment. In addition to parametric modulation[43], our category-selective analytical approach[36,44], allowed us to characterise neural responses during continuous transitions between novel and familiar sectors of a naturalistic environment. Importantly, our viewpoint-invariant analysis focused solely on positional information, which is an essential hallmark of cognitive maps[2]. Beyond identifying gradients across the hippocampal long axis, the results of our study highlighted the complementary role of the posterior medial cortex in the graded representation of spatial novelty-to-familiarity during virtual navigation. In addition to advancing our understanding of spatial information coding in the human brain, our findings may have important implications for memory disorders and the development of future generation, brain-inspired artificial agents.

Results

Modelling of spatial novelty during virtual navigation

During 7T fMRI scanning, a total of 56 participants freely navigated an open plane, circular arena with extra-boundary landmarks (e.g. trees, buildings and mountains) while performing an Object Location Memory (OLM) task (Fig. 1a, b). In the encoding phase, the participants' goal was to move through the environment via translation and rotation in order to collect six objects while memorising spatial locations for later retrieval. In total, all participants completed two encoding runs with 18 trials each, collecting every object three times per run (Fig. 1b). On average, a run took 360 s (SD = 55 s) to complete. To characterise the participants' experience of spatial novelty, the environment was divided into 100 hexagonal sectors using Voronoi tessellation, and positional time series were grouped into discrete events based on the sector occupied at each time point.

Across the two task runs, participants visited an average of 50 sectors (SD = 2), with a maximum of 18 visits (SD = 1.6) to any single sector. The time elapsed between revisits to the same sector ranged from an average minimum of 6.7 s (SD = 2.3) to an average maximum of 1300 s (SD = 310). During this naturalistic behaviour paradigm, participants spent 55% of their time translating, 24% rotating, and 21% stationary (SD = 8.2, 4, 6.3%, respectively). On average, participants travelled a total of 3200 vm (SD = 140), covering substantial portions of the 180 vm diameter circular environment. Importantly, the majority of sectors had a Rayleigh vector length that was below 0.5 (0 = total uniformity, 1 = all angles are the same; mean = 0.37, SD = 0.23), which is a measure of the uniformity of angles around a circle. This indicates that the participants' sector visits were not limited to a single visual perspective (Fig. 1c). As expected, with repeated presentation of objects across trials, participants showed a significant reduction in their navigation time indicating gradual learning of object locations (−1.74 s (95% CI [−2.06, −1.40]), Supplementary Fig. S1). Together, these results affirm the participants' familiarisation with the environment through active exploration, thus validating the quantification of a continuous spatial novelty score.

To model spatial novelty, we calculated the number of times each sector was visited and the time elapsed between visits to the same sector. Using these two metrics, an aggregate novelty score was calculated for each event in each run for each participant. Bayesian hierarchical modelling revealed a decrease in this novelty score over the course of the experiment, while participants actively explored the environment (Fig. 1d; first run: −0.48 SDs, 95% CI [−0.55, −0.41]; second run: −0.71 SDs, 95% CI [−0.75, −0.66]). As expected, the decrease in the novelty score over time was steeper in the second run of the task. Additionally, we assessed whether the novelty score correlated with changes in locomotion as participants encountered novel sectors. We found that participants spent more time being stationary and rotating in novel sectors (Supplementary Fig. S2), suggesting that these moments involved increased deliberation to process novel spatial information[45]. Using quantiles, the individual-specific spatial novelty scores were then discretised into six levels for each participant, ranging from novel to familiar (i.e. Level 1 = highly novel, Level 6 = highly familiar), for subsequent neuroimaging analyses. Areal partitioning of the environment to inner and outer circles[6] indicated that the highly novel events were uniformly distributed across the centre and periphery, which ensured that experiencing novelty was not confounded by centrality (Supplementary Fig. S3).

Mapping spatial novelty along the hippocampal long axis

Given the central role of the hippocampus in spatial navigation and novelty processing[12], our initial analysis of the 7T fMRI data focused on characterising the sensitivity of this region to systematic variations in spatial novelty/familiarity, which were quantified from participants' naturalistic behaviour during spatial navigation.

A linear contrast across the six discretised novelty levels revealed significant sensitivity of the bilateral anterior hippocampus, extending into the amygdala, to systematic changes in spatial novelty during virtual navigation (Fig. 2a and Supplementary Table S2, Cluster IDs = 193, 194). In these parts of the hippocampus, greater activity was observed while participants navigated through highly familiar sectors of the virtual reality environment, whereas mid-to-posterior portions displayed greater activity for higher spatial novelty. Additional control analyses investigating the potential role of centrality on the observed effects revealed negligible influence of this environmental factor on spatial novelty responses (Supplementary Figs. S4, S5).

https://doi.org/10.1038/s41467-025-67012-z

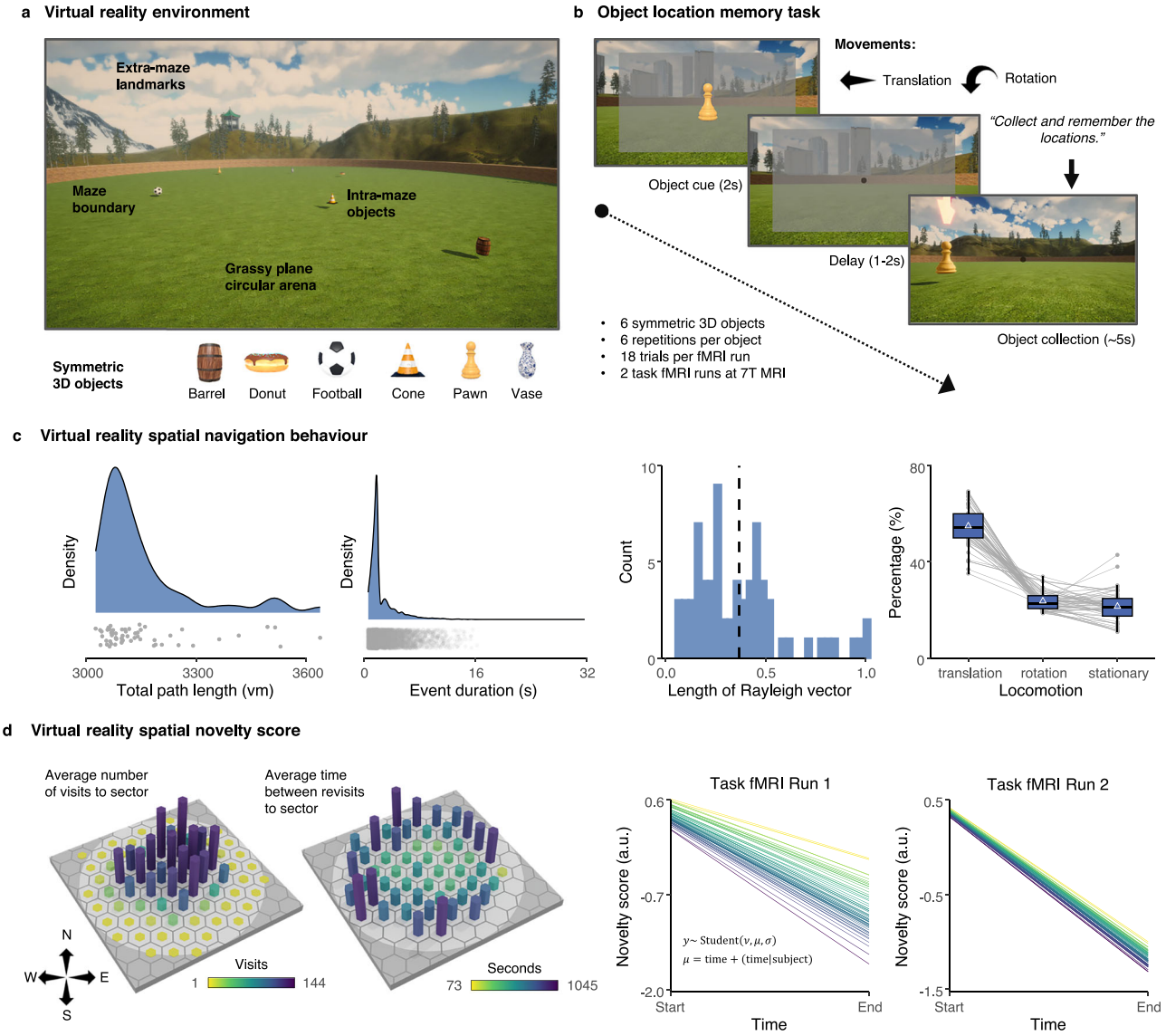

Fig. 1 | Experimental design and behavioural performance during virtual navigation. a The virtual environment designed for this experiment was a circular grassy plane arena enclosed by a 180 virtual metres (vm) diameter brick wall with extra-maze landmarks. **b** Task trials started with the presentation of a cued object image (2 s) and a variable delay (1–2 s). Participants were instructed to collect the target object and memorise its location for future retrieval. **c** During encoding, participants travelled large distances (mean = 3200 vm, SD = 140 vm, $N = 56$) with varying event durations (mean = 2.5 s, SD = 2.1 s, $N = 8755$), which are visualised as density plots with individual data points (for each participant and each event). The majority of sectors had a Rayleigh vector length below 0.5 (0 = total uniformity, 1 = all angles are the same; mean = 0.37, SD = 0.23, $N = 72$), indicating that the participants' sector visits were independent of specific viewpoints. The histogram illustrates the distribution across sectors, while the dashed black line indicates the average. Participants spent 55 % of their time translating, followed by rotating (24%) and being stationary (21 %, $N = 56$). While boxplots visualise the median (horizontal black line), hinges of the boxes denote the 25th and 75th percentiles, and whiskers extent to the most extreme values no further than 1.5 times the IQR from the hinge. The white triangle represents the mean. **d** Overall, participants actively explored the majority of the environment as indicated by 3D histograms that display the average number of discrete visits and the average time elapsed between visits across 100 hexagonal sectors. The heights and colours represent visits and seconds. These two measures were then used to calculate an aggregate novelty score for each event in each run for each participant. Bayesian hierarchical modelling revealed an expected decrease in novelty score over time (first run: −0.48 SDs, 95% CI [−0.55, −0.41]; second run: −0.71 SDs, 95% CI [−0.75, −0.66]), reflecting the participants' active encoding of the environment. Source data are provided as a Source Data file.

Our subsequent aim was to directly investigate the existence of a graded representation of spatial novelty-to-familiarity scales along the hippocampal long axis. For that purpose, we first employed a normal-based point to plane/curve projection that better captured the shape and angle of the hippocampus (Fig. 2b). A novelty preference level (Level 1: highly novel, Level 6: highly familiar) was then assigned to each hippocampal voxel based on the strength of their selective responses and voxels with the same axial position were then averaged. Using this positional information, as well as nuisance variables such as temporal signal-to-noise ratio and global signal, we predicted the average novelty versus familiarity preference while shuffling the voxel labels 100,000 times. In order to investigate hemispheric differences in graded representations[46], we included voxels from both the right and the left hippocampus in the analysis, modelling the interaction between longitudinal axis position and brain hemisphere.

When investigating novelty preference based on the minimum z-statistic, the effect of position was significantly different across the two hemispheres ($\beta = 0.022$, $\eta^2 = 0.03$, $p = 0.021$). Importantly, separate models for each hemisphere revealed that position significantly affected novelty preference in both the left ($\beta = 0.021$, $\eta^2 = 0.053$,

https://doi.org/10.1038/s41467-025-67012-z

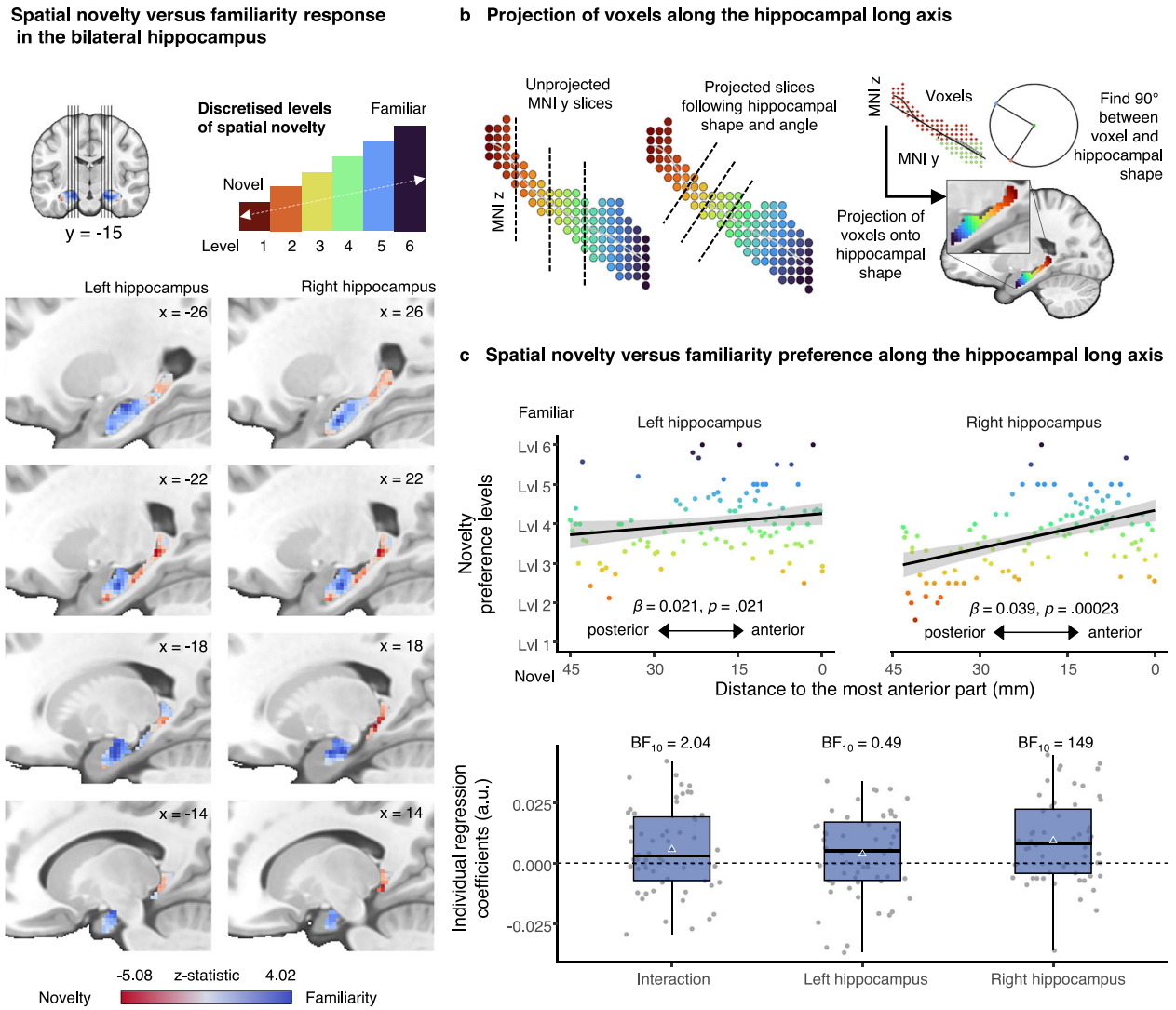

Fig. 2 | Graded representation of spatial novelty-to-familiarity scales across the hippocampal long axis. a Spatial novelty versus familiarity responses in the bilateral hippocampus. Task activation patterns and their anterior-to-posterior variation are displayed across sagittal slices for each hemisphere. While the anterior hippocampus showed significantly higher activity when participants were in familiar parts of the environment, the posterior hippocampus responded to spatial novelty (cFDRp <0.05). Unthresholded z-statistics are shown for visualisation (red = novelty, blue = familiarity). **b** To investigate graded representations along the hippocampal long axis, we developed a method that incorporates the average shape and angle of the hippocampus, by finding the right angle between the tangent and the line from each voxel to the curve. **c** Spatial novelty-to-familiarity gradients are illustrated in scatter plots for the left and right hippocampus separately. Each dot represents the average of a number of voxels with the same anterior-ness value (i.e. distance to the most anterior part in mm) based on the group-level z-statistic map ($N = 102$ for the left hemisphere and $N = 104$ for the right hemisphere). Colouring follows the six discretised novelty/familiarity levels. The black line represents the linear model's regression line with a 95% confidence interval (shaded grey area). Regression coefficients and two-tailed p values are based on the multiple linear regression models estimated via permutation, including the temporal signal-to-noise ratio as well as the global signal as covariates. This group-level analysis showed significant gradients in both the left and the right hippocampus, while a significant interaction indicated that the gradient was stronger in the right hemisphere. At the individual-level ($N = 56$), this analysis showed a significant gradient in the right hemisphere, with inconclusive evidence for a significant difference between the two hemispheres. Boxplots visualise the median (horizontal black line), hinges of the boxes denote the 25th and 75th percentiles, and whiskers extend to the most extreme values no further than 1.5 times the IQR from the hinge. The white triangle represents the mean. No adjustments were made for multiple comparisons. Source data are provided as a Source Data file.

$p = 0.021$) and right hemispheres ($\beta = 0.039$, $\eta^2 = 0.154$, $p < 0.001$), with a stronger effect observed in the right hemisphere (Fig. 2c). Together these results indicated a significant graded representation of spatial novelty-to-familiarity along the posterior to anterior axis of the bilateral hippocampus.

Similar results were replicated when using the maximum z-statistic (see Supplementary Fig. S6) and non-averaged raw voxel preference for spatial novelty levels (Supplementary Fig. S7). In order to ensure that our results were not an artefact of group-level averaging, we also estimated graded representations at the individual level. Providing converging evidence (Fig. 2c), we found significant slopes in the right hippocampus (mean $\beta = 0.0093$, SD = 0.017, $BF_{10} = 149$, d = 0.54) but not in the left hippocampus (mean $\beta = 0.0037$, SD = 0.017, $BF_{10} = 0.49$, d = 0.21). Despite these hemispheric disparities, a direct comparison between the two hemispheres yielded inconclusive evidence for a difference (mean $\beta = 0.0056$, SD = 0.017, $BF_{10} = 2.04$, d = 0.32).

In summary, our results demonstrate a spatial novelty-to-familiarity gradient, with the anterior hippocampus preferring spatial familiarity and the posterior hippocampus preferring spatial novelty. Despite stronger effects observed on the right hemisphere, evidence for a hemispheric difference in this graded representation remains inconsistent across our analyses.

https://doi.org/10.1038/s41467-025-67012-z

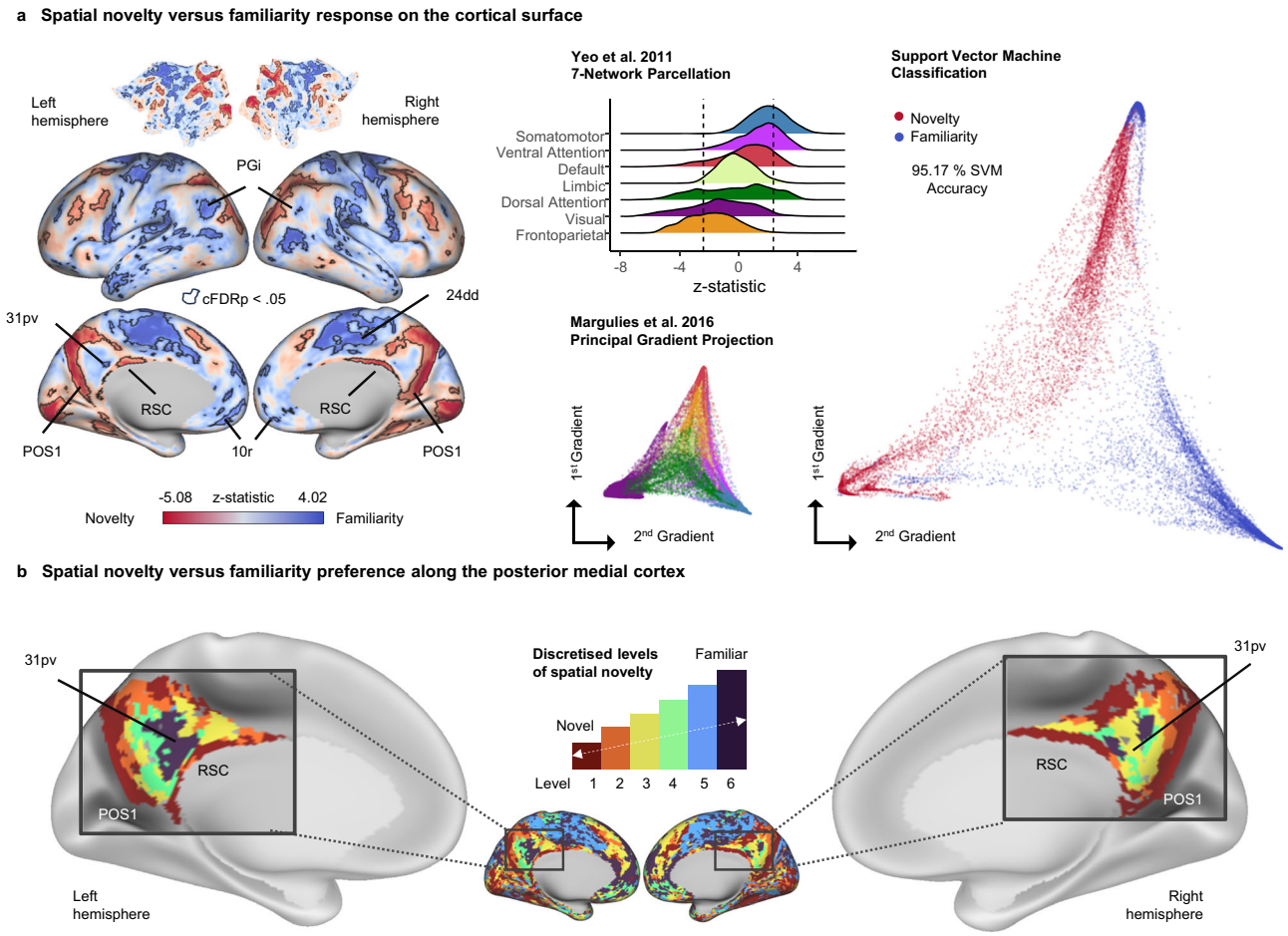

Fig. 3 | Extension of spatial novelty-to-familiarity scales to the cortical surface. **a** Novelty versus familiarity responses across the cortical surface. Top left flat maps and inflated cortical surfaces show z-statistics for novelty versus familiarity contrast (red = novelty, blue = familiarity) with black lines outlining significant clusters corrected for multiple comparisons across all grayordinates and two contrasts (cFDRp <0.05). Our analysis revealed large parts of the cortex that were sensitive to spatial novelty/familiarity, which is also evident when plotting the distributions of z-statistics across Yeo et al.[47]. 7-Network parcellation as density plots. While vertices within the frontoparietal and visual networks showed greater activity for spatial novelty, vertices within the somatomotor, ventral attention and default mode networks displayed greater activity for spatial familiarity. The vertical dashed lines represent the significance thresholds for both tails after FDR correction. In addition, projecting significant vertices onto the first two principal functional connectivity gradients reported by ref. 37 allowed the separation of novelty versus familiarity responses with high accuracy (SVM, 95.17%). Dots are coloured based on the sign of the z-statistic. For easier interpretation, the locations of the Yeo-7 networks are also visualised in the same space. **b** Applying our modified depth-first-search algorithm across the whole brain, only a bilateral region within the posterior medial cortex exhibited a graded representation of spatial familiarity to novelty, starting in the centre of a region within the default network (31pv) that lies at the border between ventral and dorsal posterior cingulate cortex and extending towards peripheral visual cortices (POS1). While the surrounding areas of the posterior medial cortex, including the retrosplenial cortex, the precuneus and the outer edges of the ventral and dorsal posterior cingulate cortex, preferred novelty, the centre of the posterior cingulate cortex preferred familiarity in a centre-surround pattern. Source data are provided as a Source Data file.

Extension of spatial novelty scales to the posterior medial cortex

Emerging evidence indicates the involvement of extra-hippocampal brain regions in spatial cognition, with multiple scales of spatial representations previously observed along the neocortex[36]. Thus, our next aim was to investigate whether graded representation of spatial novelty-to-familiarity also extended to cortical areas. For that purpose, we first assessed the sensitivity of the human cortex to systematic variations in spatial novelty.

The analysis revealed large swaths of cortical regions that were sensitive to fluctuations in spatial novelty versus familiarity (Fig. 3a). While a peak cluster in area intraparietal 0 (IP0, Cluster ID = 38) showed greater response to higher spatial novelty, a peak cluster in area 6 mp (Cluster ID = 87) illustrated a preference for greater familiarity (Supplementary Tables S1, 2). Within the posterior medial cortex, the precuneus and retrosplenial cortex primarily exhibited novelty effects, whereas the central portion of the posterior cingulate cortex showed sensitivity to spatial familiarity. When described at the level of macro-scale brain network organisation (i.e. Yeo-7 parcellation[47]), large parts of the frontoparietal and visual networks displayed significantly higher activity while participants navigated across novel parts of the virtual reality environment. On the other hand, sections within the somatomotor, ventral attention and default mode networks were significantly more active when participants navigated through familiar sectors of the virtual reality environment. Importantly, our supplementary analysis showed that regions with increased activity in response to spatial novelty also exhibited higher activity for objects that were more successfully encoded in memory. In contrast, regions responding to spatial familiarity did not show similar activity modulation based on encoding success (Supplementary Fig. S8). Together, these results corroborate previous findings highlighting the vital role played by novelty signals in memory encoding[13,48,49].

To further characterise the distribution of the spatial novelty effects across the cortical surface, we projected significant vertices onto the principal functional connectivity gradients[37]. This low-dimensional representation serves as an alternative coordinate

https://doi.org/10.1038/s41467-025-67012-z

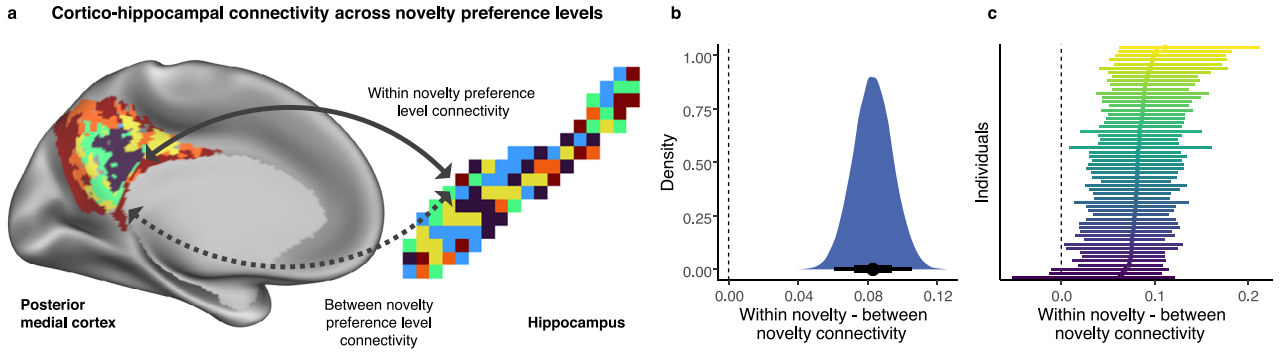

Fig. 4 | Connectivity of the hippocampus and posterior medial cortex across spatial novelty scales. a Prior work suggests that functionally related regions tend to couple more strongly at rest, reflecting their coordinated role in information processing[50]. As illustrated in a schematic, we expected stronger connectivity within the same than between different novelty levels. For this, Fisher z-transformed Pearson correlation values from a dense connectivity matrix were averaged for each level combination in the hippocampal voxels and the posterior medial cortex vertices. **b** Bayesian hierarchical regression was then used to investigate whether connectivity was higher within the same novelty level (e.g. Level 6 in hippocampus and Level 6 in posterior medial cortex) compared to between novelty levels (e.g. Level 6 in hippocampus and 4 in posterior medial cortex) while controlling for the main effects of cortical and hippocampal novelty levels. The average marginal effect at the group-level (0.0831 SDs 95% CI [0.061, 0.106]) showed a robust effect, indicating stronger connectivity for vertex-voxel pairs that shared the same versus divergent novelty preference levels. The density plot illustrates the posterior distribution of the group-level marginal effect (based on 50,000 samples). The point represents the median, while the thick and thin black line below the distribution represent the 66% and 95% quantile interval, respectively. **c** This effect was also robust at the individual level ($N = 56$). Here, average marginal effects (within the same novelty level minus between novelty levels) are visualised with the median and the 95% quantile interval for each individual separately, demonstrating that within novelty level connectivity was stronger across the vast number of participants, as indicated by the lack of overlap with zero (dashed line). Source data are provided as a Source Data file.

system that orders vertices based on intrinsic connectivity profiles instead of spatial proximity, offering a new perspective on brain organisation. When projected onto the first (unimodal to transmodal) and second (visual to somatomotor) principal gradients, a high degree of separability was observed between vertices showing novelty versus familiarity effects (4-fold SVM classification accuracy = 95.17%; Fig. 3a), indicating two complementary processing streams with distinguishable sensitivity to spatial novelty versus familiarity.

Given such separable responses along the functional connectivity gradients, our next objective was to assess the possibility of a graded representation of spatial novelty-to-familiarity scales along the cortical surface. We followed the same approach that was employed for the hippocampus, in which each vertex was assigned a novelty preference level based on the strength of its category-selective responses to distinct levels of spatial novelty. A maze-solving algorithm was then adapted to travel along the cortical surface to identify regions of interest in which novelty preference moved in a stepwise manner. Peak regions from Level 6 (highly familiar) were used as starting points for the algorithm. Only Level 5 was allowed to be skipped as no selective activity patterns were observed for this level.

Across all the peaks investigated in this analysis, graded representations were identified solely within the bilateral posterior medial cortex (Fig. 3b). This circular gradient started from a cluster within a core region of the default mode network, namely Area 31pd/31pv that showed selectivity for spatial familiarity and extended outwards in a centre-surround pattern to regions within the visual cortex such as DVT/POS1 (e.g. retrosplenial cortex) and frontoparietal network that selectively responded to spatial novelty.

To further characterise these graded representations within the posterior medial cortex, we investigated the correspondence between our task-based spatial novelty-to-familiarity responses in the cortex and the principal functional connectivity gradient[37]. Here, we found a monotone relationship where vertices preferring novelty (e.g. Level 1 vertices) had lower values on the first principal gradient compared with vertices preferring navigation through familiar sectors (e.g. Level 6 vertices; Supplementary Fig. S9). In other words, novelty preference was linked to the unimodal visual end of the first principal gradient, whereas familiarity preference was linked to the transmodal default mode end of this organisational system.

Cortico-hippocampal connectivity across spatial novelty scales

Our in-depth analysis revealed graded representations of spatial novelty-to- familiarity along both the hippocampal long axis and posterior medial cortex. A wealth of research now suggests that regions sharing similar functional specialisations are intrinsically co-organised, showing stronger resting-state coupling as a marker of coordinated processing[50]. Next, we asked whether voxels in the hippocampus showed tighter functional coupling with those vertices in the posterior medial cortex that share the same novelty/familiarity preference.

For that purpose, we analysed functional connectivity estimates based on resting-state fMRI data collected from the same participants (Fig. 4). While controlling for the mean effect of novelty levels in the hippocampus and in the posterior medial cortex, we found a significant estimated average difference when comparing pairs of within novelty versus between novelty preference levels 0.0831 SDs 95% CI [0.061, 0.106]. In other words, the parts of the hippocampus and the posterior medial cortex that shared the same preference levels for spatial novelty-familiarity were more tightly coupled in comparison to those that showed diverging preference levels.

In parallel, the anterior hippocampus aligned more strongly with the principal gradients that differentiate the default mode from other networks, than did representations in the posterior hippocampus. Mirroring our task and resting-state-based analyses, this supports a closer relationship between the anterior hippocampus and the default mode network, consistent with recent work[29,35,42,51] (Supplementary Fig. S10).

Discussion

In this study, our primary objective was to investigate how the human brain processes spatial novelty during naturalistic navigation in a virtual reality environment. Specifically, we examined whether graded representations serve as a neural mechanism for encoding spatial novelty across both the hippocampus and extra-hippocampal brain regions. Our findings revealed several key insights. First, the hippocampus exhibited significant sensitivity to systematic variations in spatial novelty, with distinct activity profiles observed across its longitudinal poles. While the bilateral anterior hippocampus showed heightened activity in response to spatial familiarity, the mid-to-posterior portions responded to spatial novelty. Crucially, we

identified a graded representation of spatial novelty-to-familiarity along the hippocampal long axis.

Beyond the medial temporal lobe, our results additionally highlighted two distinct cortical processing streams: regions within the visual and frontoparietal networks responded preferentially to spatial novelty, whereas somatomotor, ventral attention and default mode network regions displayed greater activity for familiar sectors of the environment. Importantly, we observed a graded representation of spatial novelty scales within the posterior parietal cortex, extending from a key posterior default mode network region towards visual and frontoparietal areas in a centre-surround pattern. Furthermore, we found that hippocampal and posterior parietal cortex clusters with matching novelty preferences demonstrated stronger connectivity at rest, suggesting an intrinsic functional coupling between these two gradients. Collectively, our findings indicate that graded representations of spatial novelty-to-familiarity serve as a fundamental organisational mechanism for encoding spatial information.

Converging evidence across decades of animal research has firmly established the hippocampus as a critical component of the brain's navigational circuitry[16]. In particular, the discovery of place cells and other spatially tuned neurons, such as grid cells, head direction cells and border cells, has collectively demonstrated the medial temporal lobe's essential role in representing spatial environments[1,52]. A well-documented characteristic of hippocampal function is the division of labour along its longitudinal axis. The anterior hippocampus is generally thought to process coarse and generalised spatial information, while the posterior hippocampus is implicated in detailed perceptual representations[33,40,53].

Consistent with this framework, our results show that the anterior hippocampus exhibits significant sensitivity to view-invariant processing of familiar spaces during naturalistic virtual navigation. The capacity to represent spatially coherent scenes is essential not only for recognising environments and recalling autobiographical events but also for constructing novel scenes that facilitate generalisation and imagination of future scenarios[54,55]. Supporting this view, prior research has demonstrated the anterior hippocampus' role in forming and utilising schemata, with recent studies providing evidence for schematic spatial representations in this region during virtual navigation[56–58]. Taken together, these findings underscore the anterior hippocampus' contribution to the processing of familiar spaces, a function that may be crucial for constructing cognitive maps that support efficient navigation.

However, our findings are also in contrast with some prior studies employing different experimental paradigms that have reported increased anterior hippocampal activity in response to certain types of novelty (e.g. unexpected stimuli in visual sequences) or have failed to detect familiarity-related responses in this region[17,41,59,60]. The heterogeneity of novelty (or surprise) as a concept complicates direct comparisons across studies[13], as task designs and contrasts vary substantially. This variability is reminiscent of the ongoing debate regarding the anterior-posterior distinction in processing global/coarse versus local/fine spatial information[34,56]. Nonetheless, our data are in line with the notion that the anterior hippocampus is primarily engaged by memory-based processes, whereas the posterior hippocampus is more responsive to perceptual processes such as salience-based novelty. This interpretation aligns closely with recent findings[42] demonstrating that the anterior hippocampus is preferentially activated by remembering and imagining episodic scenarios, while the posterior hippocampus shows sensitivity to salience-based novelty and transitions between task blocks. While the evidence for this distinction in virtual reality paradigms remains mixed[12,15], a general trend in the literature suggests that memory-derived novelty engages the anterior hippocampus[17,24,61,62] whereas salience-based novelty, such as target detection, activates the posterior hippocampus[18,42].

As such, our findings contribute to an emerging framework that reconciles previous inconsistencies in hippocampal function by distinguishing between memory-driven and perception-driven processing[40]. This perspective may account for why scene perception[61] and perceptual strength-based processing[63] predominantly engage the posterior hippocampus. Similarly, the findings in which the anterior hippocampus was shown to selectively activate when participants judged distances on a global scale (e.g. continents) while the posterior hippocampus was engaged for local-scale decisions (e.g. rooms), can also be interpreted as global information relying more on memory and schemata, whereas local information relying more on perception[36]. Thus, the novelty-familiarity gradient we report mirrors prior research demonstrating the sensitivity of the hippocampus to various types of novelty[17–19] while also aligning with broader physiological and functional gradients observed in receptor distributions, gene expression and pathology studies[27,28] as well as functional gradients[25,32–36]. More broadly, the presence of multiple spatial and non-spatial gradients within the hippocampus supports the proposal that this structure enables general-purpose computations through a geometric neural code that originally evolved for spatial navigation[64].

In addition to the seminal role ascribed to the hippocampus in spatial cognition, our findings further emphasise the importance of extra-hippocampal brain regions in spatial navigation[23,65]. Specifically, the retrosplenial cortex, known for allocentric positional coding[58,66,67] and the parahippocampal cortex, essential for landmark recognition[68,69], both exhibited sensitivity to spatial novelty in our virtual reality experiment. Additionally, the amygdala, traditionally associated with affective processing, showed increased activity in familiar sectors[70], reinforcing its broader role in mnemonic processing and novelty detection[59,71–74]. These results collectively suggest that a more extensive neural network contributes to distinguishing between novel and familiar sectors of an environment during spatial navigation.

Our analysis further revealed distinct patterns of novelty and familiarity representation across the cortical surface. Regions within the visual and frontoparietal networks exhibited stronger responses to novelty, whereas the somatomotor, ventral attention and default mode networks showed greater activity when navigating familiar sectors. The distinctiveness of the processing streams became even more apparent when mapped onto the principal functional connectivity gradients, an alternative coordinate system that represents a fundamental organisational architecture in the human brain[37]. The distribution of brain regions preferring spatial novelty and familiarity not only matched those that report continuous scale gradients[36] but also those that contrast novelty and memory[42,75].

Historically, the navigational neural circuitry has been primarily associated with scene-processing regions in the visual cortex, as well as transmodal cortices that are involved in salience detection, executive control and flexible cognition[76,77]. However, emerging perspectives now highlight a potential role for the default mode network in spatial cognition[24], particularly during coasting of familiar spaces[23]. This aligns with previous reports linking the default mode network to the automated application of learned rules[78] and the automatic retrieval of strongly encoded episodic and semantic memories[79], further indicating a role for this domain-general "core recollection network"[80] in the organisation of both spatial and non-spatial knowledge. As such, it will be imperative for future research to investigate the exact role of this large-scale brain network in spatial cognition and its potential relevance for effective navigation in the real world.

Crucially, our investigation of graded representations across the cortical surface revealed the representation of spatial novelty-to-familiarity scales specifically centred on the posterior medial cortex. In line with recent anatomical models[81], the ventral/dorsal portions of the posterior cingulate cortex, a key hub of the default mode network, showed a preference for highly familiar sectors of the environment. This gradually dissipated in a stepwise manner, shifting toward higher

novelty preference in the visual and frontoparietal network regions, creating a macro-scale centre-surround organisation that exhibited a similar arrangement to that of the principal functional connectivity gradients. Furthermore, our investigation of intrinsic connectivity between hippocampal and cortical gradients showed stronger connectivity between clusters with matching novelty preferences. These results align with prior reports, showing greater connectivity between anterior portions of the hippocampus and the default mode network, while posterior portions connect more strongly with visual and frontoparietal control regions[35,42,82]. This suggests that gradient-like representations, similar to those observed in connectivity-profiles[37], represent a general pattern of brain organisation that coexists alongside clear regional boundaries[83,84]. Further research will be required to assess how such regional gradients are situated within the broader macro-scale organisation of the human brain, specifically within the processing of spatial information.

Novelty processing has long been theorised to play a critical role in memory encoding[13,48,49]. Consistent with this view, regions identified as sensitive to novelty in our analysis also exhibited stronger activation during processing of more successfully encoded objects. Coupled with our finding that participants engaged in more encoding-related behaviours when encountering novel parts of the environment, these results underscore the importance of spatial novelty processing for memory formation. Unlike previous studies[49], our definitions of novelty and successful encoding were independent, as they were derived from distinct levels of analysis. This independence provides compelling evidence that novelty processing contributes directly to memory encoding rather than reflecting a methodological confound.

Despite the robustness of our findings across multiple levels of analysis, several limitations warrant consideration. First, we only assessed spatial novelty within a single environment rather than across multiple contexts. To enhance generalisability, future research should compare novelty processing both within and between environments, incorporating variations in spatial scale. Additionally, our focus was limited to linear novelty gradients, yet it is possible that certain spatial representations follow non-linear organisational principles. Further investigation is needed to explore such complexities. Moreover, several prior studies have highlighted the influence of environmental factors, such as centrality (i.e. distance to the border), on hippocampal responses[6,15]. Although we implemented controls at the experimental design stage and conducted supplementary analyses (Supplementary Figs. S4, S5), which showed minimal influence of this factor on our results, it is unlikely that the effects of these and other environmental factors can be fully disentangled from the spatial novelty-to-familiarity responses observed during naturalistic navigation. Likewise, distinctions along the hippocampal long axis have been linked to differential contributions of encoding and retrieval[85–88]. While our design sought to minimise retrieval demands and our analyses accounted for incidental memory retrieval effects, these influences cannot be completely ruled out in a naturalistic navigation paradigm with free behaviour. Future research will therefore be needed to systematically investigate how such factors map onto hippocampal representations.

In conclusion, our investigation provides novel insights into how the human brain processes spatial information. Using 7T fMRI during virtual navigation, we identified distinct functional divisions along the hippocampal long axis, with the anterior hippocampus preferentially processing familiar environments and the posterior hippocampus responding to novel spatial information. Beyond a binary distinction, we revealed continuous gradients of spatial novelty-to-familiarity encoding in both the hippocampus and posterior medial cortex. These graded representations were further supported by intrinsic connectivity patterns linking regions with similar novelty preferences, suggesting a fundamental neural principle underlying the processing of spatial information. Our results, therefore, add to the growing body of work highlighting the topographic organisation of knowledge in the human brain (e.g. semantic maps[89]) and significantly advance the understanding of hippocampal and cortical function in spatial cognition and their broader role in the formation and use of cognitive maps for navigation.

Methods

Participants

All experimental procedures complied with the Declaration of Helsinki, Ethical Principles for Medical Research Involving Human Participants, and were approved by the ISTBI institutional review board (AF/SC-21/20210604). Participants provided informed consent prior to study commencement and were compensated 100 RMB per hour. In line with the inclusion/exclusion criteria, participants were right-handed healthy individuals with normal or corrected-to-normal vision and with no known history of psychiatric or neurological disorders. A total of seven participants were excluded from data analysis because of technical errors or performance issues in the virtual navigation task. The final dataset included 56 participants, who completed all the required cognitive, behavioural and neuroimaging-based assessments: age range = 20-37 years, mean age = 24 years (SD = 2.8), female/male ratio = 35/21.

Experimental procedures

The experiment required two separate visits to the Zhangjiang International Brain Imaging Centre, Fudan University. On Day 1, participants were first familiarised with navigating the virtual reality environment using an independent cognitive paradigm and a practice version of the main experimental task. Subsequently, a comprehensive neuroimaging assessment was conducted using a 3T MRI to acquire anatomical, resting-state fMRI data and task fMRI runs (not analysed as part of this study). Post-scanning, participants completed an automated battery of cognitive tasks and questionnaires. On Day 2, following a short practice session outside the scanner, 7T fMRI data were acquired using the Object Location Memory task with novel hidden object locations. The average interval between the two neuroimaging sessions was 12 days (SD = 13).

Virtual reality environment and experimental task design

The core experimental paradigm was based on prior studies that used virtual reality environments to investigate the neural basis of spatial navigation in humans[6,7,55,90]. Our environment consisted of a round, grassy, open plane arena, surrounded by a brick wall (diameter 180 vm) and extra-maze landmarks (mountains, clouds, trees, buildings, etc.). Participants navigated the arena using a button box with three degrees of freedom (forward translation, left and right rotation) at constant translation and rotation speeds of 10 vm/s and 50°/s, respectively. A total of six 3D intra-maze objects were used, chosen for their relative symmetry along their vertical axes to avoid view-dependent confounds. Trial order, object locations, heading directions and starting positions were randomised based on a set of pre-defined spatial constraints (Supplementary Notes S1).

The open-source object location memory task was programmed using the video game development platform Unity3D, in which the unity experiment framework (UXF[91]) was employed to handle data recording and experimental structure (e.g. trials and blocks). The main 7T Object Location Memory task comprised two alternating run types: encoding and retrieval. This multi-faceted experiment was designed with several subcomponents to investigate spatial learning and memory in a controlled virtual reality environment using high-resolution fMRI. In line with our main research question on spatial novelty, we focused our fMRI analysis solely on the encoding runs, which were specifically designed to encourage active exploration of a new spatial layout, devoid of goal-oriented memory retrieval. The participants' objective within the encoding runs was to collect and memorise the spatial locations of six objects for later retrieval. In each of the two

encoding runs, six objects were presented three times in a pre-randomised order across a total of 18 trials. Each trial started with the presentation of a cue image of the target object placed on top of a grey transparent panel for 2 s (Fig. 1b). This was followed by a variable delay period of 1–2 s where only the round fixation marker was visible on the screen. After this delay phase, participants could navigate towards the object, which was visible throughout the whole trial and highlighted with a vertical arrow. The collection of the target object ended the trial, which was followed by a variable inter-trial interval (ITI) that lasted 1–2 s. On average, each trial lasted 20 s (SD = 3.1) with a total completion time of 360 s (SD = 55) for each task run.

MRI data acquisition

A high-quality neuroimaging data acquisition procedure was set up and optimised based on the Human Connectome Project (HCP). In compliance with the requirements of the HCP minimal pre-processing pipeline[92] relevant data were acquired to aid multi-modal registration of MRI images. While anatomical measures (T1w, T2w) and resting-state fMRI data were collected using a 3T Magnetom Prisma MRI scanner (Siemens, Erlangen, Germany) with a 32-channel head coil, task fMRI data were acquired using 7T Magnetom Terra MRI scanner (Siemens, Erlangen, Germany) with a 1-channel transmit and 32-channel receive array (1Tx/32Rx) head coil (Nova Medical, Wilmington, MA, USA).

At 3T, we collected whole-brain anatomical images using a T1-weighted MPRAGE sequence (0.7-mm isotropic resolution, TR = 2400 ms, TE = 2.02 ms, TI = 1000 ms, flip angle = 8°, bandwidth = 270 Hz per pixel, no partial Fourier, in-plane acceleration factor (iPAT) = 2, TA = 7.4 min per scan) and a T2-weighted SPACE sequence (0.7-mm isotropic resolution, TR = 3200 ms, TE = 564 ms, BW = 744 Hz per pixel, no partial Fourier, iPAT = 2, TA = 8.2 min per scan). In addition, a pair of resting-state fMRI runs was acquired with anterior and posterior phase encoding polarity using a 2D multiband (MB) gradient-recalled echo (GRE) echo-planar imaging (EPI) sequence (2.0-mm isotropic resolution, TR = 800 ms, TE = 37 ms, flip angle = 52°, bandwidth = 270 Hz per pixel, multiband acceleration factor = 8, 488 volumes, TA = 6.4 min). With the aim of aiding post-hoc distortion correction, we also obtained a dual-echo gradient and a pair of spin echo images with AP and PA phase encoding polarity.

For the main Object Location Memory task fMRI runs at 7T, data acquisition was performed using an MB GRE-EPI sequence comparable to 3T but with higher spatial resolution (1.6 mm isotropic resolution, TR = 1000 ms, TE = 22.2 ms, flip angle = 45°, multiband acceleration factor = 5, average of 410 and 370 volumes for the two runs, respectively). Associated field maps with matching geometry and echo spacing were also acquired to aid in post-hoc distortion correction of functional imaging data. During task fMRI runs, the experimental paradigm was presented on an MRI-compatible rear projection screen using a PROPixx projector (VPixx Technologies Inc., Canada). The display was situated inside the scanner bore, which participants viewed through a mirror attached to the head coil at a 45° angle. The display-to-mirror distance was measured to be 202.5 cm (resolution 1920 × 1080 at 120 Hz, visual angle 6°). All behavioural responses were recorded using a four-button box.

MRI data pre-processing

The pre-processing of neuroimaging data was performed via Quantitative Neuroimaging Environment and Toolbox (Qunex[93]) using a Singularity-based containerised version of the HCP minimal pre-processing pipeline[92].

To summarise this process that is extensively documented elsewhere, T1w and T2w structural images were first corrected for distortions, co-registered and warped to the MNI-152 template using a combination of FMRIB Software Library (FSL) linear and non-linear image registration tools. The FreeSurfer recon-all pipeline was then employed to generate grey and white matter tissue segmentations, cortical surface models and subcortical segmentation masks. The cortical ribbon based on the pial and white matter surface boundaries was combined with the subcortical voxels to generate a CIFTI 'grayordinate' space for each individual.

Functional images were motion corrected via alignment to the single-band reference images, masked to exclude signal from non-brain tissue, corrected for distortions, registered to structural images and normalised to the MNI-template (2 mm isotropic) in a single transform step that minimised interpolation costs. The anatomically defined grey matter cortical ribbon was then employed to convert fMRI data to the CIFTI matrix. While the cortical surfaces were registered to the group average HCP atlas (fsLR 32k space) using surface-based non-linear deformation, the MNI-152 registered subcortical volume component of the CIFTI image was isolated using FreeSurfer-defined subcortical segmentation. Additionally, ICA-Fix[94,95] was used to remove noise components from concatenated runs of resting-state and task-based fMRI data. Finally, a multi-modal surface matching (MSMAll) algorithm[96,97] functionally aligned all fMRI data using a combination of myelin and resting-state maps. For task activation analyses, additional smoothing was applied to achieve a final 4 mm FHWM spatial smoothing across both cortical and subcortical data, whereas the gradient identification and resting-state analyses were performed on the native 2 mm smoothed version of the data. Subsequent handling of CIFTI files for the neuroimaging data analyses and visualisations were carried out using *ciftiTools*[98] and Connectome Workbench[99].

Behavioural analyses

Hierarchical Bayesian regression models. For data analysis, several Bayesian hierarchical regression models were fit using the R package brms[100,101]. Unless stated otherwise, we used the same procedure for all models, including the use of full random effects (slopes and intercepts) for individuals. All models were fit using ten chains each with 10,000 iterations, half of which were used for warm-up. All of them converged with a maximum $\hat{R}$ of 1. Posterior predictive cheques were carried out to evaluate the appropriateness of the response distribution (Supplementary Fig. S13). For priors, we used $N(0, 1)$ for all fixed effects, while for all other parameters, we used the default options. Such generic and weakly informative priors were chosen to regularise unexpectedly large effects[102]. Non-categorical predictor variables were all scaled to have a mean of 0 and a SD of 0.5. Based on these hierarchical models, average marginal effects[103] using default comparisons were estimated, incorporating group-level uncertainty on the response scale. Thus, effects were reported in vm, seconds or SDs (if the predicted variable had been scaled), respectively.

To investigate learning during the encoding phase of the experiment (Supplementary Fig. S1), we modelled navigation times in seconds (without scaling) as a function of the number of times the current object has been presented using a lognormal response distribution. In order to control for the minimum distance participants had to travel using the optimal path, we also included the distance between the start and the object location in this model.

Quantification of spatial novelty. In order to investigate the neural representation of spatial novelty, a continuous novelty score was calculated for each task event based on the participants' virtual navigation behaviour in the object location memory task. To achieve this, we divided the virtual reality environment into 100 sectors using Voronoi tessellation, which categorised each time point/position based on the closest seed. This resulted in hexagons with an in-diameter of 20 vm. In order to reduce computational load, we down-sampled the data from 60 to 5 Hz and defined events based on all time points that spanned the same sector using run length encoding. For each event, we calculated a novelty score, which integrates two measures of spatial novelty: (1) the

number of visits and (2) the elapsed time since the last visit to a particular sector.

The final vector of novelty scores for each participant was quantified by averaging the two measures after mean-centring and scaling to one standard deviation across all events and across all runs within each participant. Only data from the two encoding runs were included in the fMRI analysis; however, navigational behaviour in the first retrieval run were also taken into account when calculating the novelty score for the second encoding run. In order not to bias our analysis towards initial encounters with a sector, for which an elapsed time is not defined, these events were excluded from subsequent neural analyses.

Within each run, the novelty score was predicted by elapsed time since the onset of the run. To account for wide tails in the data, a student distribution was used. The novelty score was scaled to have a mean of 0 and an SD of 1.

MRI data analysis

The main objective of our functional neuroimaging data analysis was to investigate the neural response to spatial novelty in the human brain and, in particular, to assess the graded representation of spatial novelty along the hippocampal long axis and across the cortical mantle as a potential coding mechanism. For that purpose, our initial analysis focused on unravelling brain regions with activity profiles that were reliably sensitive to systematic variations in spatial novelty during the Object Location Memory task.

To achieve this, we first discretised the spatial novelty score for each participant separately into six levels (i.e. Level 1 = highly novel, Level 6 = highly familiar) based on quantiles. Using HCP task fMRI analysis pipelines and FSL FEAT routines, we then modelled each novelty level as a separate regressor in a general linear model (GLM). Events within each novelty level were entered as variable epochs[104] and regressors were convolved with FSL's double-gamma (phase 0°) HRF using pre-whitening. Cue and delay periods were modelled as regressors of no interest, while the ITI periods were included as part of the implicit baseline. The contrast used for task activation analysis was a parametric modulation in the form of a linear change in novelty, which allowed us to identify peak regions of interest that were sensitive to spatial novelty and familiarity. To estimate group-level effect sizes and significance, we used Permutation Analysis of Linear Models (PALM) through sign flipping[105]. All results were corrected for multiple comparisons at the grayordinate level and across contrasts (negative and positive) via false discovery rate (FDR) at the $p < 0.05$ level of significance[106].

All surface-based results were displayed on top of the inflated S1200 group average MSMAll-registered surfaces from the HCP, while subcortical results were overlaid onto MNI-152 structural brain images. Dense cortical results were reported with reference to the HCP multimodal parcellation of the brain (HCP-MMP v1.0)[107]. Results were further characterised at the network level using the Yeo-7-network parcellation[47] and the principal functional connectivity manifolds[37] for which the maps were extracted from the BrainStat[108] toolbox. Significant cortical vertices were projected onto a 2D space defined by the first two principal gradients. The degree of separation was quantified by predicting whether a vertex showed a novelty or a familiarity effect based on the position in this alternative 2D space using a support vector machine with a radial kernel. For this analysis, the vertices were split into training (75%) and test (25%) sets.

Graded representation analysis. To investigate graded representations of spatial novelty-to-familiarity along the hippocampal long axis and across the cortical mantle, we performed an additional GLM analysis akin to the procedures employed in ref. 36. In this GLM and similar to previous work[44], each novelty level was contrasted against the average of all other levels to identify voxels/vertices that selectively responded to each level of novelty/familiarity. The z-statistic maps of the group-level results were then used to categorise each subcortical voxel and cortical vertex for their novelty preference. This was achieved by assigning a value between 1 (highly novel) and 6 (highly familiar) based on the strength of responses (i.e. z-statistics) observed for each level of novelty/familiarity. The minimum z-value was used as the main definition of the strongest response since our a priori region of interest, i.e. the hippocampus, largely showed negative responses to novelty (higher activity for familiar sectors). The minimum z-statistic was interpreted as the reverse of level preferences i.e. if a vertex showed the lowest z-statistic for Level 1 (novel) it was considered as evidence for preference to Level 6 (familiar).

Hippocampal graded representation analysis. For the hippocampal analysis, we used bilateral hippocampus masks based on the FreeSurfer subcortical segmentations included in the CIFTI format. Building upon prior investigations[32,36], we first aimed to account for the curvature of the hippocampus along the y-coordinates of the MNI space. For that purpose, a normal-based point to plane/curve projection was employed (see Fig. 2b). A function for the average shape of the right and the left hippocampus was estimated by regressing the MNI y-coordinate onto the MNI z-coordinate via a generalised additive model (GAM) and the shrinkage version of a cubic regression spline (bs = cs). With this continuous function, we were able to project each y-value onto the average shape, which involved finding the tangent of the voxel location and the function. At the extreme ends of the hippocampus, where a tangent was not available, the original function value was used instead. Finally, the cumulative Euclidean distance was calculated for each point from anterior-to-posterior, resulting in an anterior-ness value.

After this projection, we averaged the novelty preference of each voxel with the same position value. On average, there were 7.6 (SD = 3) voxels per unique position along the anterior-to-posterior axis. Lastly, we used this position to predict the average preference value, which could vary between 1 and 6. To ensure gradients did not simply arise from data quality differences along the hippocampal long axis, we also included the temporal signal-to-noise ratio (tSNR) and the global signal averaged across runs and participants as co-variates in the model. To test for potential hemispheric differences[46], we first added both hemispheres into a model and included hemisphere as a factor along with its interaction with position (i.e. preference ~ position * hemisphere + tSNR + GS). In the absence of a significant interaction effect, we averaged across hemispheres (i.e. preference ~ position + tSNR + GS). Significance of the hippocampal gradient was assessed by shuffling the novelty preference labels 100,000 times and comparing the regression coefficients of the simple linear models with the null distribution that was generated through the shuffling procedure. *P* values were calculated by fitting a function to the null distribution via log-spline density estimation. This technique makes use of the whole null distribution, and it is particularly useful to estimate the density of distribution tails, leading to a more robust estimation of the *p* value.

In order to ensure that the reported results are not due to artefacts of averaging at the group-level, we also repeated the graded representation analysis at the individual level, calculating regression coefficients for each participant separately and then submitting these coefficients to Bayesian *t*-tests against zero. Individual-level tSNR and global signal measures, averaged across the two runs, were entered as co-variates. The Bayes factors for two-tailed *t*-tests were calculated using the BayesFactor package[109] with the standard r-scale prior of $\sqrt{2}/2$.

Cortical graded representation analysis. In addition to the hippocampal long axis, we aimed to investigate graded representations of spatial novelty scales across the cortical mantle. For that purpose, we developed a custom depth-first search algorithm, which is able to travel

along the cortical surface respecting its folding pattern. The algorithm started from peak vertices of the Level 6 (highly familiar) clusters identified in our novelty selectivity analysis, and at each step could only move to a neighbouring vertex. The same results could be achieved using peak vertices of the Level 1 (highly novel) clusters. Vertices are neighbours when they share a face in the 32k Conte69 mesh. To uncover gradients, the algorithm was only allowed to walk from one vertex to a neighbouring vertex with either the same level or a level of N-1. Since Level 5 was mostly absent in our cortical analysis, the algorithm was allowed to skip this level. We used one vertex per Level 6 cluster as a starting point for the algorithm. Potential gradients were then inspected visually and discarded if they only arose via tangential connections (e.g. via a single vertex). Similarly, tangentially connected vertices were manually removed from the remaining gradients.

Functional connectivity analysis. To quantify the correspondence between hippocampal and cortical gradients, we estimated dense connectivity matrices (59412 × 1559) between each cortical vertex and each hippocampal voxel for each participant. The connectivity matrices were estimated using Pearson correlation of the corresponding BOLD time series based on two runs of resting-state fMRI data obtained from the same participants (AP/PA). After applying Fisher's z-transformation, connectivity values were averaged for each novelty level and hemisphere (left/right hippocampus and left/right posterior medial cortex). To investigate whether voxels in the hippocampus were more strongly connected to vertices in the cortex that share the same novelty preference level, we used Bayesian hierarchical modelling with full random effects. This model included a binary variable indicating whether the two levels were the same or different within a pair. Additionally, we included the novelty preference level in the hippocampus and in the cortex to capture mean differences between novelty levels (i.e. connectivity ~ cortex_level + HC_level + is_same_level) with full random slopes and intercepts for each individual. The Fisher z-transformed connectivity values were scaled to have a mean of 0 and an SD of 1. Effects are therefore reported in terms of SDs.

Reporting summary

Further information on research design is available in the Nature Portfolio Reporting Summary linked to this article.

Data availability

The raw data generated in this study cannot be made publicly available due to restrictions imposed by institutional ethics approval and the informed consent obtained from study participants. Individual-specific brain maps (e.g., fMRI response estimates) are available under restricted access to qualified researchers, contingent upon approval of a data use agreement and compliance with institutional ethics guidelines. Access requests should be submitted to the corresponding author (Prof. Deniz Vatansever, deniz@fudan.edu.cn) and will be reviewed by the institutional data access committee. Requests will typically receive a response within 4 weeks. Approved data will be made available for non-commercial research purposes for a period of 5 years following approval. All group-level statistical brain maps supporting the findings of this study are publicly available at the BALSA repository (https://balsa.wustl.edu/study/0w1gk). The data used to generate the figures in this study are provided in the accompanying Source Data file. Source data are provided with this paper.

Code availability

All custom code used to reproduce the analyses reported in this study, including statistical comparisons and the depth-first search algorithm, is available at (https://github.com/cognizelab/SpaNovVR)[110]. Detailed information on data pre-processing procedures can be found in the QuNex documentation (https://qunex.readthedocs.io/en/latest/wiki/UsageDocs/RunningPreprocessHCP.html). In addition, a fully customisable and user-friendly version of the Unity-based virtual reality task developed for this study is publicly available at (https://github.com/JAQuent/Object-Location-Memory-Task)[111]. This task was designed to be accessible to researchers without programming experience, and all data analysed in this manuscript were collected using Version 2.1.1 of this task.

References

1. Behrens, T. E. J. et al. What is a cognitive map? Organizing knowledge for flexible behavior. *Neuron* **100**, 490–509 (2018).
2. Jeffery, K. J. The mosaic structure of the mammalian cognitive map. *Learn Behav*. https://doi.org/10.3758/s13420-023-00618-9 (2024).
3. O'Keefe, J. & Dostrovsky, J. The hippocampus as a spatial map. Preliminary evidence from unit activity in the freely-moving rat. *Brain Res.* **34**, 171–175 (1971).
4. Malanchini, M. et al. Evidence for a unitary structure of spatial cognition beyond general intelligence. *npj Sci. Learn.* **5**, 9 (2020).
5. Coughlan, G. et al. Toward personalized cognitive diagnostics of at-genetic-risk Alzheimer's disease. *Proc. Natl. Acad. Sci. USA* **116**, 9285–9292 (2019).
6. Kunz, L. et al. Reduced grid-cell-like representations in adults at genetic risk for Alzheimer's disease. *Science* **350**, 430–433 (2015).
7. Stangl, M. et al. Compromised grid-cell-like representations in old age as a key mechanism to explain age-related navigational deficits. *Curr. Biol.* **28**, 1108–1115.e6 (2018).
8. Newton, C. et al. Entorhinal-based path integration selectively predicts midlife risk of Alzheimer's disease. *Alzheimer's Dement.* **20**, 2779–2793 (2024).
9. Jafarpour, A. & Spiers, H. Familiarity expands space and contracts time. *Hippocampus* **27**, 12–16 (2017).
10. Teng, E. & Squire, L. R. Memory for places learned long ago is intact after hippocampal damage. *Nature* **400**, 675–677 (1999).
11. Annese, J., Klaming, R., Haase Alasantro, L. & Feinstein, J. S. A case of severe anterograde amnesia in the era of smartphone technology. *J. Clin. Exp. Neuropsychol.* **45**, 498–512 (2023).
12. Kaplan, R., Horner, A. J., Bandettini, P. A., Doeller, C. F. & Burgess, N. Human hippocampal processing of environmental novelty during spatial navigation. *Hippocampus* **24**, 740–750 (2014).
13. Quent, J. A., Henson, R. N. & Greve, A. A predictive account of how novelty influences declarative memory. *Neurobiol. Learn. Mem.* **179**, 107382–107382 (2021).
14. Howard, L. R., Kumaran, D., Olafsdottir, H. F. & Spiers, H. J. Double dissociation between hippocampal and parahippocampal responses to object-background context and scene novelty. *J. Neurosci.* **31**, 5253–5261 (2011).
15. Doeller, C. F., King, J. A. & Burgess, N. Parallel striatal and hippocampal systems for landmarks and boundaries in spatial memory. *Proc. Natl. Acad. Sci. USA* **105**, 5915–5920 (2008).
16. O'Keefe, J. & Nadel, L. *The Hippocampus as a Cognitive Map* (Oxford Univ. Press, 1978).
17. Tulving, E., Markowitsch, H. J., Craik, F. I. M., Habib, R. & Houle, S. Novelty and familiarity activations in PET studies of memory encoding and retrieval. *Cereb. Cortex* **6**, 71–79 (1996).
18. Knight, R. T. Novelty detection model. *Nature* **383**, 256–259 (1996).
19. Kumaran, D. & Maguire, E. A. Novelty signals: a window into hippocampal information processing. *Trends Cogn. Sci.* **13**, 47–54 (2009).
20. Jeewajee, A., Lever, C., Burton, S., O'Keefe, J. & Burgess, N. Environmental novelty is signaled by reduction of the hippocampal theta frequency. *Hippocampus* **18**, 340–348 (2008).
21. Barry, C., Heys, J. G. & Hasselmo, M. E. Possible role of acetylcholine in regulating spatial novelty effects on theta rhythm and grid cells. *Front. Neural Circuits* **6**, 1–13 (2012).

22. Schomaker, J. Unexplored territory: Beneficial effects of novelty on memory. *Neurobiol. Learn. Mem.* https://doi.org/10.1016/j.nlm.2019.03.005 (2019).
23. Patai, E. Z. & Spiers, H. J. The versatile wayfinder: prefrontal contributions to spatial navigation. *Trends Cogn. Sci.* **25**, 520–533 (2021).
24. Zeidman, P. & Maguire, E. A. Anterior hippocampus: the anatomy of perception, imagination and episodic memory. *Nat. Rev. Neurosci.* **17**, 173–182 (2016).
25. Kjelstrup, K. B. et al. Finite scale of spatial representation in the hippocampus. *Science* **321**, 140–143 (2008).
26. Poppenk, J., Evensmoen, H. R., Moscovitch, M. & Nadel, L. Long-axis specialization of the human hippocampus. *Trends Cogn. Sci.* **17**, 230–240 (2013).
27. Strange, B. A., Witter, M. P., Lein, E. S. & Moser, E. I. Functional organization of the hippocampal longitudinal axis. *Nat. Rev. Neurosci.* **15**, 655–669 (2014).
28. Ortega-Cruz, D. et al. Three-dimensional histology reveals dissociable human hippocampal long-axis gradients of Alzheimer's pathology. *Alzheimer's Dement.* **20**, 2606–2619 (2024).
29. Zheng, A. et al. Parallel hippocampal-parietal circuits for self- and goal-oriented processing. *Proc. Natl. Acad. Sci. USA* **118**, e2101743118 (2021).
30. Leferink, C. A. et al. Organization of pRF size along the AP axis of the hippocampus and adjacent medial temporal cortex is related to specialization for scenes versus faces. *Cereb. Cortex* **34**, bhad429 (2024).
31. Thorp, J. N., Gasser, C., Blessing, E. & Davachi, L. Data-driven clustering of functional signals reveals gradients in processing both within the anterior hippocampus and across its long axis. *J. Neurosci.* **42**, 7431–7441 (2022).
32. Bouffard, N. R. et al. Single voxel autocorrelation uncovers gradients of temporal dynamics in the hippocampus and entorhinal cortex during rest and navigation. *Cereb. Cortex* **33**, 3265–3283 (2023).
33. Brunec, I. K. et al. Multiple scales of representation along the hippocampal anteroposterior axis in humans. *Curr. Biol.* **28**, 2129–2135.e6 (2018).
34. Evensmoen, H. R. et al. From details to large scale: the representation of environmental positions follows a granularity gradient along the human hippocampal and entorhinal anterior–posterior axis. *Hippocampus* **25**, 119–135 (2015).
35. Eichert, N. et al. Hippocampal connectivity patterns echo macroscale cortical evolution in the primate brain. *Nat. Commun.* **15**, 5963 (2024).
36. Peer, M., Ron, Y., Monsa, R. & Arzy, S. Processing of different spatial scales in the human brain. *eLife* **8**, e47492 (2019).
37. Margulies, D. S. et al. Situating the default-mode network along a principal gradient of macroscale cortical organization. *Proc. Natl. Acad. Sci. USA* **113**, 12574–12579 (2016).
38. Tarder-Stoll, H., Baldassano, C. & Aly, M. The brain hierarchically represents the past and future during multistep anticipation. *Nat. Commun.* **15**, 9094 (2024).
39. Wang, X., Margulies, D. S., Smallwood, J. & Jefferies, E. A gradient from long-term memory to novel cognition: transitions through default mode and executive cortex. *Neuroimage* **220**, 117074 (2020).
40. Irish, M. & Vatansever, D. Rethinking the episodic-semantic distinction from a gradient perspective. *Curr. Opin. Behav. Sci.* **32**, 43–49 (2020).
41. Strange, B. A., Fletcher, P. C., Henson, R. N. A., Friston, K. J. & Dolan, R. J. Segregating the functions of human hippocampus. *Proc. Natl. Acad. Sci. USA* **96**, 4034–4039 (1999).
42. Angeli, P. A., DiNicola, L. M., Saadon-Grosman, N., Eldaief, M. C. & Buckner, R. L. Specialization of the human hippocampal long axis revisited. *Proc. Natl. Acad. Sci. USA* **122**, e2422083122 (2025).
43. Mumford, J. A., Poline, J.-B. & Poldrack, R. A. Orthogonalization of Regressors in fMRI Models. *PLoS ONE* **10**, e0126255 (2015).
44. Stigliani, A., Weiner, K. S. & Grill-Spector, K. Temporal processing capacity in high-level visual cortex is domain specific. *J. Neurosci.* **35**, 12412–12424 (2015).
45. Lancia, G. L., Eluchans, M., D'Alessandro, M., Spiers, H. J. & Pezzulo, G. Humans account for cognitive costs when finding shortcuts: an information-theoretic analysis of navigation. *PLoS Comput. Biol.* **19**, e1010829 (2023).
46. Jordan, J. T. The rodent hippocampus as a bilateral structure: a review of hemispheric lateralization. *Hippocampus* **30**, 278–292 (2020).
47. Yeo, B. T. T. et al. The organization of the human cerebral cortex estimated by intrinsic functional connectivity. *J. Neurophysiol.* **106**, 1125–1165 (2011).
48. Tulving, E. & Kroll, N. Novelty assessment in the brain and long-term memory encoding. *Psychonomic Bull. Rev.* **2**, 387–390 (1995).
49. Kim, H. Differential neural activity in the recognition of old versus new events: an activation likelihood estimation meta-analysis. *Hum. Brain Mapp.* **34**, 814–836 (2013).
50. Smith, S. M. et al. Correspondence of the brain's functional architecture during activation and rest. *Proc. Natl. Acad. Sci. USA* **106**, 13040–13045 (2009).
51. Grady, C. L. Meta-analytic and functional connectivity evidence from functional magnetic resonance imaging for an anterior to posterior gradient of function along the hippocampal axis. *Hippocampus* **30**, 456–471 (2020).
52. Epstein, R. A., Patai, E. Z., Julian, J. B. & Spiers, H. J. The cognitive map in humans: spatial navigation and beyond. *Nat. Neurosci.* **20**, 1504–1513 (2017).
53. Sekeres, M. J., Winocur, G. & Moscovitch, M. The hippocampus and related neocortical structures in memory transformation. *Neurosci. Lett.* **680**, 39–53 (2018).
54. Addis, D. R. & Schacter, D. L. Constructive episodic simulation: temporal distance and detail of past and future events modulate hippocampal engagement. *Hippocampus* **18**, 227–237 (2008).
55. Horner, A. J., Bisby, J. A., Zotow, E., Bush, D. & Burgess, N. Grid-like processing of imagined navigation. *Curr. Biol.* **26**, 842–847 (2016).
56. Kim, M. & Maguire, E. A. Hippocampus, retrosplenial and parahippocampal cortices encode multicompartment 3D space in a hierarchical manner. *Cereb. Cortex* **28**, 1898–1909 (2018).
57. Sekeres, M. J., Schomaker, J., Nadel, L. & Tse, D. To update or to create? The influence of novelty and prior knowledge on memory networks. *Philos. Trans. R. Soc. B* **379**, 20230238 (2024).
58. Peer, M. & Epstein, R. A. The human brain uses spatial schemas to represent segmented environments. *Curr. Biol.* **31**, 4677–4688.e8 (2021).
59. Blackford, J. U., Buckholtz, J. W., Avery, S. N. & Zald, D. H. A unique role for the human amygdala in novelty detection. *Neuroimage* **50**, 1188–1193 (2010).
60. Kumaran, D. & Maguire, E. A. An unexpected sequence of events: mismatch detection in the human hippocampus. *PLoS Biol.* **4**, e424 (2006).
61. Zeidman, P., Mullally, S. L. & Maguire, E. A. Constructing, perceiving, and maintaining scenes: hippocampal activity and connectivity. *Cereb. Cortex* **25**, 3836–3855 (2015).
62. Grunwald, T., Lehnertz, K., Heinze, H. J., Helmstaedter, C. & Elger, C. E. Verbal novelty detection within the human hippocampus proper. *Proc. Natl. Acad. Sci. USA* **95**, 3193–3197 (1998).

63. Aly, M., Ranganath, C. & Yonelinas, A. P. Detecting changes in scenes: the hippocampus is critical for strength-based perception. *Neuron* **78**, 1127–1137 (2013).
64. Bellmund, J. L. S., Gärdenfors, P., Moser, E. I. & Doeller, C. F. Navigating cognition: spatial codes for human thinking. *Science* **362**, eaat6766 (2018).
65. Baumann, O. & Mattingley, J. B. Extrahippocampal contributions to spatial navigation in humans: a review of the neuroimaging evidence. *Hippocampus* **31**, 640–657 (2021).
66. Epstein, R. A. & Vass, L. K. Neural systems for landmark-based wayfinding in humans. *Philos. Trans. R. Soc. B Biol. Sci.* **369**, 20120533 (2014).
67. Chen, X., Wei, Z. & Wolbers, T. Repetition suppression reveals cue-specific spatial representations for landmarks and self-motion cues in the human retrosplenial cortex. *eNeuro* **11**, ENEURO.0294-23.2024 (2024).
68. Janzen, G., Jansen, C. & Turennout, M. van. Memory consolidation of landmarks in good navigators. *Hippocampus* **18**, 40–47 (2008).
69. Wegman, J. & Janzen, G. Neural encoding of objects relevant for navigation and resting state correlations with navigational ability. *J. Cogn. Neurosci.* **23**, 3841–3854 (2011).
70. LeDoux, J. The amygdala. *Curr. Biol.* **17**, R868–R874 (2007).
71. Halgren, E. et al. Endogenous potentials generated in the human hippocampal formation and amygdala by infrequent events. *Science* **210**, 803–805 (1980).
72. Fried, I., MacDonald, K. A. & Wilson, C. L. Single neuron activity in human hippocampus and amygdala during recognition of faces and objects. *Neuron* **18**, 753–765 (1997).
73. Rutishauser, U., Ross, I. B., Mamelak, A. N. & Schuman, E. M. Human memory strength is predicted by theta-frequency phase-locking of single neurons. *Nature* **464**, 903–907 (2010).
74. Balderston, N. L., Schultz, D. H. & Helmstetter, F. J. The human amygdala plays a stimulus specific role in the detection of novelty. *Neuroimage* **55**, 1889–1898 (2011).
75. Kwon, Y. H. et al. Situating the salience and parietal memory networks in the context of multiple parallel distributed networks using precision functional mapping. *Cell Rep.* **44**, 115207 (2025).
76. Herweg, N. A. & Kahana, M. J. Spatial representations in the human brain. *Front. Hum. Neurosci.* **12**, 297 (2018).
77. Kravitz, D. J., Saleem, K. S., Baker, C. I. & Mishkin, M. A new neural framework for visuospatial processing. *Nat. Rev. Neurosci.* **12**, 217–230 (2011).
78. Vatansever, D., Menon, D. K. & Stamatakis, E. A. Default mode contributions to automated information processing. *Proc. Natl. Acad. Sci. USA* **114**, 12821–12826 (2017).
79. Vatansever, D., Smallwood, J. & Jefferies, E. Varying demands for cognitive control reveals shared neural processes supporting semantic and episodic memory retrieval. *Nat. Commun.* **12**, 2134 (2021).
80. Rugg, M. D. & Vilberg, K. L. Brain networks underlying episodic memory retrieval. *Curr. Opin. Neurobiol.* **23**, 255–260 (2013).
81. Foster, B. L. et al. A tripartite view of the posterior cingulate cortex. *Nat. Rev. Neurosci.* **24**, 173–189 (2023).
82. Dalton, M. A., D'Souza, A., Lv, J. & Calamante, F. New insights into anatomical connectivity along the anterior–posterior axis of the human hippocampus using in vivo quantitative fibre tracking. *eLife* **11**, e76143 (2022).
83. Glasser, M. F. et al. The Human Connectome Project's neuroimaging approach. *Nat. Neurosci.* **19**, 1175–1187 (2016).
84. Petersen, S. E., Seitzman, B. A., Nelson, S. M., Wig, G. S. & Gordon, E. M. Principles of cortical areas and their implications for neuroimaging. *Neuron* **112**, 2837–2853 (2024).
85. Spaniol, J. et al. Event-related fMRI studies of episodic encoding and retrieval: Meta-analyses using activation likelihood estimation. *Neuropsychologia* **47**, 1765–1779 (2009).
86. Kim, H. Encoding and retrieval along the long axis of the hippocampus and their relationships with dorsal attention and default mode networks: the HERNET model. *Hippocampus* **25**, 500–510 (2015).
87. Fritch, H. A. et al. The anterior hippocampus is associated with spatial memory encoding. *Brain Res.* **1732**, 146696 (2020).
88. Tang, L. et al. Differential functional connectivity in anterior and posterior hippocampus supporting the development of memory formation. *Front. Hum. Neurosci.* **14**, 204 (2020).
89. Huth, A. G., de Heer, W. A., Griffiths, T. L., Theunissen, F. E. & Gallant, J. L. Natural speech reveals the semantic maps that tile human cerebral cortex. *Nature* **532**, 453–458 (2016).
90. Doeller, C. F., Barry, C. & Burgess, N. Evidence for grid cells in a human memory network. *Nature* **463**, 657–661 (2010).
91. Brookes, J., Warburton, M., Alghadier, M., Mon-Williams, M. & Mushtaq, F. Studying human behavior with virtual reality: the unity experiment framework. *Behav. Res.* **52**, 455–463 (2020).
92. Glasser, M. F. et al. The minimal preprocessing pipelines for the Human Connectome Project. *Neuroimage* **80**, 105–124 (2013).
93. Ji, J. L. et al. QuNex—An integrative platform for reproducible neuroimaging analytics. *Front. Neuroinform.* **17**, 1104508 (2023).
94. Griffanti, L. et al. ICA-based artefact removal and accelerated fMRI acquisition for improved resting state network imaging. *Neuroimage* **95**, 232–247 (2014).
95. Salimi-Khorshidi, G. et al. Automatic denoising of functional MRI data: combining independent component analysis and hierarchical fusion of classifiers. *Neuroimage* **90**, 449–468 (2014).
96. Robinson, E. C. et al. MSM: a new flexible framework for multimodal surface matching. *NeuroImage* **100**, 414–426 (2014).
97. Robinson, E. C. et al. Multimodal surface matching with higher-order smoothness constraints. *Neuroimage* **167**, 453–465 (2018).
98. Pham, D. D., Muschelli, J. & Mejia, A. F. ciftiTools: a package for reading, writing, visualizing, and manipulating CIFTI files R. *Neuroimage* **250**, 118877 (2022).
99. Marcus, D. S. et al. Informatics and data mining tools and strategies for the human connectome project. *Front. Neuroinform.* **5**, 4 (2011).
100. Bürkner, P.-C. brms: an R package for Bayesian multilevel models using Stan. *J. Stat. Softw.* **80**, 1–28 (2017).
101. Bürkner, P.-C. Advanced Bayesian multilevel modeling with the R package brms. *R. J.* **10**, 395–411 (2018).
102. Gelman, A., Jakulin, A., Pittau, M. G. & Su, Y.-S. A weakly informative default prior distribution for logistic and other regression models. *Ann. Appl. Stat.* **2**, 1360–1383 (2008).
103. Arel-Bundock, V., Greifer, N. & Heiss, A. How to interpret statistical models using **marginaleffects** for R and Python. *J. Stat. Soft.* **111**, 1–32 (2024).
104. Grinband, J., Wager, T. D., Lindquist, M., Ferrera, V. P. & Hirsch, J. Detection of time-varying signals in event-related fMRI designs. *Neuroimage* **43**, 509–520 (2008).
105. Winkler, A. M., Ridgway, G. R., Webster, M. A., Smith, S. M. & Nichols, T. E. Permutation inference for the general linear model. *Neuroimage* **92**, 381–397 (2014).
106. Alberton, B. A. V., Nichols, T. E., Gamba, H. R. & Winkler, A. M. Multiple testing correction over contrasts for brain imaging. *Neuroimage* **216**, 116760 (2020).
107. Glasser, M. F. et al. A multi-modal parcellation of human cerebral cortex. *Nature* **536**, 171–178 (2016).
108. Larivière, S. et al. BrainStat: a toolbox for brain-wide statistics and multimodal feature associations. *Neuroimage* **266**, 119807 (2023).
109. Morey, R. D. & Rouder, J. N. BayesFactor: computation of Bayes factors for common designs (2018).
110. Quent, J. A. et al. Graded encoding of spatial novelty scales in the human brain. *Zenodo* https://doi.org/10.5281/ZENODO.17517993 (2025).

111. Quent, J. A. & Vatansever, D. Object location memory task build with Unity3D. *Zenodo* https://doi.org/10.5281/ZENODO.17482414 (2025).

Acknowledgements

This study was funded by the Ministry of Science and Technology of China, STI2030-Major Projects (2022ZD0207900) awarded to D.V. and by the National Natural Science Foundation of China (32250410282), via the China Postdoctoral Science Foundation (2022M720818) as well as funding received from the State Key Laboratory of Medical Neurobiology and MOE Frontiers Center for Brain Science, Fudan University awarded to J.A.Q. We would also like to thank the staff at the Zhangjiang International Brain Imaging Centre for their continuous help and support, and Andrew Heiss for his advice on the interpretation of marginal effects. Finally, we extend our sincere gratitude to Matthew F. Glasser and Essa Yacoub for their support in helping us optimise the HCP data acquisition protocols for our site.

Author contributions

J.A.Q., L.S., X.L., Y.S., H.W. and D.V. contributed to the conception and design of the work. J.A.Q. created the Unity3D programme that is used in this study. J.A.Q., L.S., X.L., Y.S., W.Y. and D.V. collected the data, which was analysed by D.V. and J.A.Q., who then wrote the first draft of the manuscript, which was then revised by all the authors.

Competing interests

The authors declare no competing interests.

Additional information

Supplementary information The online version contains supplementary material available at https://doi.org/10.1038/s41467-025-67012-z.

Correspondence and requests for materials should be addressed to Deniz Vatansever.

Peer review information *Nature Communications* thanks Haley Fritch, and the other, anonymous, reviewer(s) for their contribution to the peer review of this work. A peer review file is available.